Lawrence Berkeley National Laboratory
Lawrence Berkeley National Laboratory

Title

Identification of Severe Multiple Contingencies in Electric Power Systems

Permalink

https://escholarship.org/uc/item/7dc709dq

Authors

Donde, Vaibhav
Lopez, Vanessa
Lesieutre, Bernard
et al.

Publication Date

2008-06-16

Identification of Severe Multiple Contingencies in Electric Power Systems

Vaibhav Donde, *Member, IEEE,* Vanessa López, Bernard Lesieutre, *Senior Member, IEEE,*
Ali Pinar, *Member, IEEE,* Chao Yang and Juan Meza

Abstract— **In this work, we propose a computationally feasible approach to detect severe multiple contingencies. We pose a contingency analysis problem using a nonlinear optimization framework, which enables us to detect the fewest possible transmission line outages resulting in a system failure of specified severity, and the most severe system failure caused by removing a specified number of transmission lines from service. Illustrations using a three bus system and the IEEE 30 bus system aim to exhibit the effectiveness of the proposed approach.**

I. INTRODUCTION

Robust operation of a power grid requires anticipation of unplanned component outages that, if not adequately considered, could lead to dramatic and costly blackouts. Planning and operating criteria are designed in order that "the interconnected power system shall be operated at all times so that general system instability, uncontrolled separation, cascading outages, or voltage collapse, will not occur as a result of any single contingency or multiple contingencies of sufficiently high likelihood" [1]. Additional more specific criteria help to achieve this famous $N-1$ criterion in practice. In this paper we consider the potential effects of the loss of multiple elements. Specifically, we pose the following two related optimization problems: 1) minimize the number of failure events that will necessitate a minimum amount of (specified) loss of load to maintain the integrity of the grid, and 2) calculate the maximum loss of load that would be required to survive a (specified) limited number of events, in any possible combination. For example, we could identify a minimum number of events that would require, for instance, loss of 1,000 MW of load, or we might calculate the most load shedding (and location) for any $N-3$ scenario. We believe these "worst-case" analyses of the more general $N-k$ problem are interesting in their own right. They can provide planners and operators more confidence in the security of the system beyond the $N-1$ requirement. Furthermore we recognize that we now operate under conditions in which we are concerned

about the possibility of purposeful and malicious $N-k$ scenarios. Such concerns may be best addressed by identifying $N-k$ scenarios that have severe consequences.

In this paper we consider the problem in a static sense through the examination of operating points in relation to the feasibility boundary of the power flow equations. We note that the severity of the events we identify could be different when dynamics are considered. Analysis of the power flow feasibility boundary has received considerable attention in the literature. Most notably it has been widely studied in terms of the use of bifurcation theory to calculate margins for secure operation relative to voltage collapse and dynamic instability. Many articles discuss this general topic (see [6] and references therein, for an overview); the most relevant to the present work are those that calculate a minimum distance to the feasibility boundary from an operating point (for a fixed network topology) [3], [9], [10], [12], [20]. This past work has also established the geometrical interpretations of a direction of best load shedding strategy in the space of load powers. For instance, Alvarado, Dobson and Hu [3] computed the point on the feasibility boundary closest to the present operating point, that is, the minimum change in power injections that would result in operation at the edge of feasibility. This closest point on the feasibility boundary provided a measure of the security margin for the given network topology, thereby providing a direction in the load parameter space that could optimally move the present operating point away from the feasibility boundary. In other words, it provided the best direction for load shedding, if the need to do so arose. Our approach is motivated by those interpretations. Moreover, we allow the network topology to change in order to incorporate transmission line failures.

Our primary contribution in this paper is to propose a method for identifying the least possible network changes (removal of transmission lines) that result in operating point infeasibility, such that the amount of minimum load shedding required for a feasible operation is greater than a user-defined threshold. Thus we deal with changes in network topology and the operating point simultaneously, within the same mathematical framework. The amount of required load shedding provides a measure of the severity of the event.

Specifically we work with a nonlinear optimization problem in terms of both network active and reactive powers and address it through a two stage analysis. In the first stage, we force the feasibility boundary to move past the nominal operating point (rendering it infeasible) by a user-specified distance, through alterations to the network. We allow a relaxation of

line parameters to incorporate the network alterations, in a similar manner as in [13], where the authors parameterized line admittances to study the effect of parameter variation on the power flow solution. The relaxation provides us a way to identify a few multiple (possibly partial) line outages that result in a severe system failure. This information obtained from the first stage is further processed in the second stage, wherein the $N - k$ analysis is performed by only considering the lines identified in the first stage. Given that such lines are typically few in number, the computational burden of the $N - k$ analysis in the second stage is far less than when all lines in the system are considered.

A similar problem of multiple contingency identification has been addressed by other researchers using analysis tools other than parameter relaxation. Salmeron, Wood and Baldick [21] employed a bilevel optimization framework along with mixed-integer programming to analyze the security of electric grid under terrorist threat. The critical elements of the grid were identified by maximizing the long-term disruption in the power system operation caused by terrorist attacks based upon limited offensive resources. The bilevel programming framework has also been used by Arroyo and Galiana [4]. In all these formulations the optimization framework appears promising for such types of problems where the critical system elements that make the system vulnerable to failures must be identified.

We emphasize that we pursue a deterministic, worst-case framework for this problem because we would like to antici-pate events that include those arising from malicious design. For a probabilistic approach to $N - k$ analysis for naturally occurring events, the reader may consider the stochastic ap-proach suggested in [8].

The static collapse of power systems is closely associated with its network topology. Our previous work [11] showed that an approximate power flow description provides a way to relate static collapse with graph partitioning using spectral graph theory. Grijalva and Sauer [15], [16] related topological cuts with the static collapse based on branch complex flows. He et. al. [17] used a voltage stability margin index to identify weak locations in a power network. Although the connections of static collapse with graph theory are useful and interesting in their own right, they remain approximate and qualitative at this stage and are not discussed further in this paper.

II. Problem Description

Conceptually, we aim to identify a small set of transmission lines in the network whose removal from service would minimally necessitate a reduction in load to avoid a potentially severe blackout, such that this minimal reduction in load would be significant. In order to be able to give a measure of the severity of the loss of these lines, we consider the minimum load lost after the failure occurs. Thus, we pose the fundamental question: what is the least altered network topology that makes the power flow infeasible at the nominal load distribution, and for which the minimum amount of load required to be shed to make the power flow feasible again is greater than some specified severity threshold?
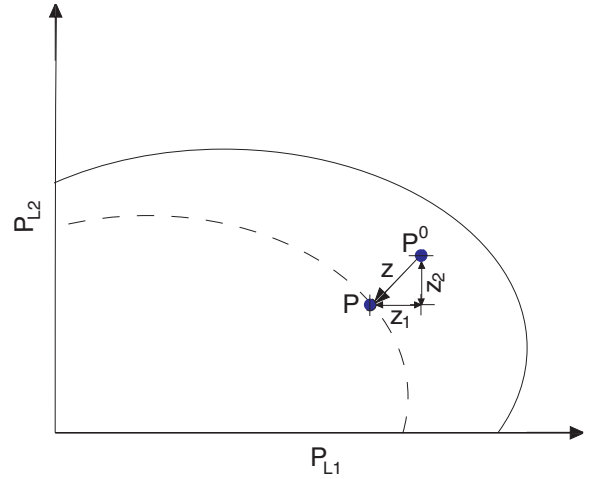

Fig. 1. Schematic view of load shedding process in the space of active load powers.

A schematic view of the load shedding process is provided in Figure 1, for a power network having constant power factor loads. The solid-lined curve represents the nominal power flow feasibility boundary when all the lines are in service. The nominal operating point P^0 lies within the feasible region of operation. When a few lines are removed from service, the feasible region shrinks and the boundary moves to the one shown as a dashed-line. The minimal load shedding strategy moves the original operating point P^0 to an operating point P that lies on the new feasibility boundary. The amount of the total load shedding, for instance, $z_1 + z_2$, corresponds to a measure of severity. Note that the feasibility boundaries may be non-convex in general, although they appear convex in the schematic representation (Figure 1).

In our analysis we consider a lossless power system network having m buses (nodes) and n lines (branches). Let P and Q be, respectively, vectors whose components are given by the active and reactive power injections at the buses. Due to the lossless character of the system, we have $\sum_{i=1}^{m} P_i = 0$, however, $\sum_{i=1}^{m} Q_i > 0$ as part of the reactive power is consumed in the network.

We note that reducing the admittance of any transmission line in the system to zero is equivalent to removing the line from service. We thus model line outages in the system by associating a set of indicator variables γ_i, $i = 1, \ldots, n$, with the line admittances and define the *modified admittance* of line i as the product of the admittance of line i with $(1 - \gamma_i)$. Then $\gamma_i = 1$ corresponds to the i-th line being removed from service, while $\gamma_i = 0$, which results in the modified admittance being equal to the nominal admittance, indicates that the line is in service.

Representing the network angle variables and voltage mag-nitudes by vectors θ and V, respectively, and letting B denote a diagonal matrix with the value of the line susceptances on its diagonal[1], the active and reactive power flow equations (with

---

[1]It is assumed for simplicity that the lines are lossless and shunt elements are absent. However the mathematical framework and the formulations pro-posed in later sections do not require this assumption.

modified admittances) can be written in matrix form as

$$A^T EB(I - \Gamma)\sin(A\theta) = P \tag{1}$$

$$-|A|^T EB(I - \Gamma)\cos(A\theta) + d = Q, \tag{2}$$

where A is the branch-node incidence matrix of the network graph and $|A|_{i,j} = |A_{i,j}|$, E is a diagonal matrix with

$$E_{i,i} = \exp((|A|\ln V)_i), \quad i = 1, \ldots, n,$$

I is the identity matrix, Γ is a diagonal matrix with

$$\Gamma_{i,i} = \gamma_i, \quad i = 1, \ldots, n,$$

d is defined by

$$d_i = V_i^2 \times (A^T B(I - \Gamma)A)_{i,i}, \quad i = 1, \ldots, m,$$

and $\sin(A\theta)$ denotes a vector whose i-th component is equal to $\sin((A\theta)_i)$. Similar notation is used to define $\cos(A\theta)$ and $\ln V$. Refer to [22] for more details on this model.

Most work documented in the literature in this context assumes the notion of a slack bus. The choice of the slack bus is typically arbitrary and it serves to supply network losses. Moreover, in the event of load shedding or load pick up, the slack bus is assumed to provide the net reduction or increment in the loads. It is well known, but often understated, that the results depend upon the choice of the slack bus. In this study, we use a *distributed slack bus*, where the net reduction in load due to load shedding is accounted for by every generator in the system by lowering their respective dispatches in proportion to their generating capacities. This eliminates the aspect of arbitrariness that the results contain when a particular bus is used as a slack bus[2]. This choice of distributed slack is motivated by the presence of droop governor controls on generators in which the response to a disturbance is distributed in a uniform manner among the generators. In the WECC system, for example, generators have 5% droop governor controls [2].

We note that due to the incorporation of a single unified distributed slack mechanism in our framework, all the generators in the system are redispatched in proportion to their nominal dispatches in response to load shedding, even when line failures result in system islanding (disconnected groups or partitions). Multiple distributed slack mechanisms would be more appropriate while dealing with cases when there is partitioning of the graph underlying the system network. Such an approach can be easily followed once the partitioning details are known. However we note that the analysis presented in this paper does not explicitly address issues related with system islanding and graph partitioning.

A. Power Flow Model, Load Shedding and Distributed Slack

Suppose that the system has m_g PV (generator) buses and m_l PQ (load) buses, such that the total buses are $m = m_g + m_l$. Let P_{pv}^0 and P_{pq}^0 be the vectors of active power injections at PV and PQ buses, respectively, at the original operating point P^0. Let $z \in \mathbb{R}^{m_l}$ be a vector representing a reduction in the active load powers due to load shedding. In general, some

PQ buses in the network will not have any load connected to them. In other words, such buses will have no load shedding activity associated with them. Corresponding components of the vector z are set to zero. It is assumed that the loads are constant power factor loads, so that the relationship $Q_{pq}^0 = M P_{pq}^0$ holds, where Q_{pq}^0 represents a vector of reactive power injections at PQ buses and M is a diagonal matrix. Hence, the reduction in reactive load powers is equal to Mz. In the space of active load powers, the vector z provides a direction for load shedding, whose components are schematically represented in Figure 1.

Note that all the elements of z are nonnegative, which is consistent with the sign convention (power injections are positive) and that the loads are only allowed to be shed. Due to the adopted notion of a distributed slack bus and the lossless character of the network, the net reduction in the active power load due to load shedding, i.e., $e^T z$, where $e = [1 \ 1 \ \ldots \ 1]^T \in \mathbb{R}^{m_l}$, is accounted for by a reduction in injection at every PV bus in proportion to their nominal generation dispatch[3]. The net reduction in active power injections at PV buses is given by the product $k P_{pv}^0$, where k is a (nonpositive) scalar. It follows from the conservation of active power that we must have $e^T z + k e^T P_{pv}^0 = 0$, therefore

$$k = -\frac{e^T z}{e^T P_{pv}^0}. \tag{3}$$

Finally, we assume here that generator voltage controls act to maintain voltage magnitudes at the PV buses at their nominal values; one need only consider the reactive power equations in (2) corresponding to PQ buses. Then, using (1)–(2), the power flow description at the new operating point P that is achieved after load shedding is given by

$$F_{pv}^P(\theta, V, \gamma) - (P_{pv}^0 + k P_{pv}^0) = 0 \tag{4}$$

$$F_{pq}^P(\theta, V, \gamma) - (P_{pq}^0 + z) = 0 \tag{5}$$

$$F_{pq}^Q(\theta, V, \gamma) - M(P_{pq}^0 + z) = 0, \tag{6}$$

where k is as in (3), $F_{pv}^P(\theta, V, \gamma)$ and $F_{pq}^P(\theta, V, \gamma)$ denote, respectively, the left-hand side from (1) corresponding to PV and PQ buses, and $F_{pq}^Q(\theta, V, \gamma)$ represents the left-hand side from (2) corresponding to PQ buses. For a given network topology (i.e., for fixed γ), the system of equations (4)–(6) geometrically represents an m_l-manifold in the space of variables (θ, V, z).

We remark that no active power balance equation is omitted in the power flow description (4)–(6), and thus no angle reference is provided. As a result, the power flow Jacobian

$$J = \begin{bmatrix} \frac{\partial F}{\partial \theta} & \frac{\partial F}{\partial V} \end{bmatrix} \tag{7}$$

has a *trivial* zero eigenvalue with $w_0 = [e^T \ \mathbf{0}^T]^T$ as the corresponding left eigenvector, where $e = [1 \ 1 \ \ldots \ 1]^T \in \mathbb{R}^m$, $w_0 \in \mathbb{R}^{m+m_l}$, and F denotes the left-hand side of (4)–(6). This is also apparent from the structure of (1)–(2) and the fact that the sum of the elements in each row of the incidence

---

[2]The notion of a distributed slack is used in [7], [23] for other applications.

[3]However, note that our approach is general enough to allow other distributed slacks.

matrix A is equal to zero. Note that w_0 satisfies

$$\frac{\partial F^T}{\partial z} w_0 = 0. \tag{8}$$

B. Obtaining a (Locally) Best Load Shedding Strategy

Referring to Figure 1, a best load shedding strategy is sought that moves the initial operating point P^0 to a new operating point P, such that a minimum amount of load is lost. Results in the literature related to this topic have employed a 2-norm notion of distance to a feasible operating point, see for example [5]. In practice, since our emphasis is on minimum load shedding, it is more appropriate to express our distance in a 1-norm sense. That is, we are more interested in the simple sum of lost load than the sum of squared lost load.

Typically the 2-norm measure is more amenable to mathematical analysis than the 1-norm. The 1-norm measure introduces an aspect of non-smoothness in the analysis, and thus may increase the complexity of the problem. As mentioned in Section II-A, in the present case however, note that every load is only allowed to be shed as opposed to being increased. This requires all the elements of z to have the same sign, in particular they need to be all nonnegative in the present framework. This observation greatly reduces the complexity that the problem would encounter otherwise, and simplifies $\|z\|_1$ to $e^T z$ (which would otherwise be $e^T |z|$). To determine such a load shedding strategy, consider the following optimization problem,

$$\min_{\theta, V, z} \quad e^T z \tag{9}$$

$$\text{s.t.} \quad F(\theta, V, z) = 0, \tag{10}$$

$$P_{pq}^0 \leq P_{pq}^0 + z \leq 0 \tag{11}$$

$$V_{min} \leq V \leq V_{max} \tag{12}$$

$$-\pi/2 \leq A\theta \leq \pi/2 \tag{13}$$

where (10) denotes the system (4)–(6) for a given network topology (i.e., for fixed γ), such that it does not have a solution at $z = 0$. Inequality constraints (11)–(13) ensure that the variables are within bounds. Note, in particular, that (11) ensures the validity of this formulation by enforcing nonnegativity of elements of vector z. It also ensures that the upper limit on the amount of load shedding is defined by the nominal load, thus preventing the loads to act as generators. Voltage magnitudes at PQ buses are bounded by upper and lower limits V_{max} and V_{min}, respectively, as indicated by (12). This constraint ensures that the voltages are within acceptable limits, even after load shedding. With a good choice of V_{min}, this constraint also serves to exclude low voltage (steady state unstable) solutions from consideration. Constraint (13) guarantees that the phase angles across the transmission lines are in a range acceptable for a steady state stable operation of the power system.

The Lagrangian corresponding to (9)–(13) is

$$\mathcal{L} = z^T e + \lambda^T F(\theta, V, z) + \mu_1^T(-z) + \mu_2^T(P_{pq}^0 + z)$$
$$+ \mu_3^T(V_{min} - V) + \mu_4^T(V - V_{max})$$
$$+ \mu_5^T(-\pi/2 - A\theta) + \mu_6^T(A\theta - \pi/2). \tag{14}$$

where λ and $\mu_1, \ldots, \mu_6$ are vectors of Lagrange multipliers. Optimal solutions to this problem satisfy the following Karush-Kuhn-Tucker conditions,

$$e + \frac{\partial F^T}{\partial z} \lambda - \mu_1 + \mu_2 = 0 \tag{15}$$

$$J^T \lambda + \begin{bmatrix} -A^T \mu_5 + A^T \mu_6 \\ -\mu_3 + \mu_4 \end{bmatrix} = 0 \tag{16}$$

$$\mu_1 \cdot z = 0 \tag{17}$$

$$\mu_2 \cdot (P_{pq}^0 + z) = 0 \tag{18}$$

$$\mu_3 \cdot (V_{min} - V) = 0 \tag{19}$$

$$\mu_4 \cdot (V - V_{max}) = 0 \tag{20}$$

$$\mu_5 \cdot (\pi/2 + A\theta) = 0 \tag{21}$$

$$\mu_6 \cdot (A\theta - \pi/2) = 0 \tag{22}$$

$$\mu_1, \cdots, \mu_6 \geq 0, \tag{23}$$

along with (10)–(13). Thus the vector z that provides the best load shedding strategy is obtained by solving (10) and (15)–(22), while honoring the inequalities (11)–(13) and (23). The notation "$\cdot$" in (17)–(22) is used to indicate component-wise multiplication of associated vectors.

When the inequality constraints (11)–(13) are inactive, we have $\mu_1, \ldots, \mu_6 = 0$. Referring to (16), this results in $J^T \lambda = 0$, which in turn makes λ a left eigenvector of J corresponding to its zero eigenvalue. Note that J must have an extra (nontrivial) zero eigenvalue as $\lambda = w_0$ does not satisfy (15) and (8) simultaneously. In other words, λ equals w, where w is a left eigenvector of J corresponding to its nontrivial zero eigenvalue. For this case, it is insightful to appreciate the geometrical interpretation of (15)–(16). Consider a hyperplane tangent to the manifold defined by (10). Vectors $(\delta\theta, \delta V, \delta z)$ on that tangent hyperplane satisfy

$$J \begin{bmatrix} \delta\theta \\ \delta V \end{bmatrix} + \frac{\partial F}{\partial z} \delta z = 0. \tag{24}$$

Premultiplying with the eigenvector w^T results in

$$w^T J \begin{bmatrix} \delta\theta \\ \delta V \end{bmatrix} + w^T \frac{\partial F^T}{\partial z} \delta z = 0, \tag{25}$$

However, as the first term in (25) vanishes to zero, we must have $\left(\frac{\partial F}{\partial z} w\right)^T \delta z = 0$. This implies that the normal to the power flow feasibility boundary at (θ, V, z) is given by $\frac{\partial F^T}{\partial z} w$. It also follows from (15) that, this normal aligns with e when the inequality constraints are inactive.

C. Relaxation on Line Admittance Coefficients

Recall that our goal is to identify a small number of transmission lines whose removal from service leads to a significant system failure, where line outages are modeled via the concept of modified admittance coefficients γ, as described at the beginning of Section II. Realistically only two situations are possible, namely, the i-th line is in service ($\gamma_i = 0$) or it is out of service ($\gamma_i = 1$). This introduces an aspect of discreteness in the analysis framework and any optimization problem formulation that involves $\gamma_i \in \{0, 1\}$ would result in an mixed-integer nonlinear programming problem. We note

that such problems are more difficult to handle than ones involving continuous variables.

We address this issue by relaxing the variable vector γ in the first stage of our analysis, and allowing its elements to take continuous values between 0 and 1. In other words, we allow partial line outages by letting

$$\gamma_i \in [0,1], \quad i = 1, \ldots, n. \tag{26}$$

Note that the discussion on obtaining the best load shedding strategy as in Section II-B is applicable for any fixed network topology (as long as the network remains connected). Thus it holds valid for situations when the lines are partially removed from service.

D. A Constrained Optimization Problem

To pose the contingency screening problem, the first stage of analysis uses a constrained optimization framework that employs the mechanisms of best load shedding strategy, distributed slack and partial line outages, described in the previous sections. Note that we seek to move both the original operating point P^0 and the power flow feasibility boundary. This boundary is moved past P^0 such that the minimum load shedding required to move P^0 to a different operating point lying on the new boundary is greater than the minimum desired severity of the blackout. Mathematically, the problem takes the following form,

$$\min_{\theta, V, z, \gamma, \mu_1, \ldots, \mu_6, \lambda} e^T \gamma \tag{27}$$

$$\text{s.t.} \quad F(\theta, V, z, \gamma) = 0 \tag{28}$$

$$e + \frac{\partial F^T}{\partial z} \lambda - \mu_1 + \mu_2 = 0 \tag{29}$$

$$J^T \lambda + \begin{bmatrix} -A^T \mu_5 + A^T \mu_6 \\ -\mu_3 + \mu_4 \end{bmatrix} = 0 \tag{30}$$

$$\mu_1 \cdot z = 0 \tag{31}$$

$$\mu_2 \cdot (P_{pq}^0 + z) = 0 \tag{32}$$

$$\mu_3 \cdot (V_{min} - V) = 0 \tag{33}$$

$$\mu_4 \cdot (V - V_{max}) = 0 \tag{34}$$

$$\mu_5 \cdot (\pi/2 + A\theta) = 0 \tag{35}$$

$$\mu_6 \cdot (A\theta - \pi/2) = 0 \tag{36}$$

$$\mu_1, \cdots, \mu_6 \geq 0 \tag{37}$$

$$P_{pq}^0 \leq P_{pq}^0 + z \leq 0 \tag{38}$$

$$V_{min} \leq V \leq V_{max} \tag{39}$$

$$-\pi/2 \leq A\theta \leq \pi/2 \tag{40}$$

$$0 \leq \gamma \leq 1 \tag{41}$$

$$e^T z \geq S_{min}. \tag{42}$$

Constraints (28) denotes the power flow equations (10), now with γ as an additional variable. Together, constraints (28)–(40) are the Karush-Kuhn-Tucker conditions as obtained in Section II-B; they are repeated here for clarity. Constraint (41) follows from the relaxation on γ. Constraint (42) ensures the total amount of load shed is greater than S_{min}, a positive-valued user defined parameter that indicates the minimum desired severity of the blackout.

By virtue of the distributed slack mechanism, all the generators contribute to the load shedding in the same proportion. This ensures that all the generators must reduce (not increase) their dispatches to account for load shedding, thus in turn ensuring that their upper dispatch capacity limits are not hit. This also guarantees that all generators will reach the lower dispatching limit assumed as zero simultaneously, when all the load in the system is shed. Thus a constraint that limits generator dispatches is unnecessary and hence is not included in the set of constraints (28)–(42).

In the present formulation, we aim to find the least number of partial line outages that result in a failure having severity greater than S_{min}. Another related formulation that can address our network vulnerability problem is where one aims to find the maximum possible failure severity when at most L_{max} number of lines are removed from service. Although both these formulations carry the same conceptual flavor, they are different problems depending upon the values that the user defined parameters S_{min} and L_{max} take. Mathematically, the latter formulation has the same structure as (27)–(42), except that the objective is now replaced by

$$\max_{\theta, V, z, \gamma, \mu_1, \ldots, \mu_6, \lambda} e^T z, \tag{43}$$

and the constraint (42) is replaced by

$$e^T \gamma \leq L_{max}, \tag{44}$$

while keeping other constraints intact.

Using either formulation (27)–(42) or (43)–(44), the critical lines for system security are identified as the ones that have non-zero γ's associated with them. In the second stage of our analysis, only such lines are considered for an $N - k$ study, where N is the number of lines identified and k may take values from 1 through N.

III. EXAMPLES

To illustrate the application of the ideas discussed in Section II, we first consider a three bus system (Figure 2), followed by the IEEE 30 bus system (Figure 7).

A. Three Bus System

This small system is convenient for an easy graphical visualization of results and to highlight the main aspects of our formulation. Consider the network as shown in Figure 2 that has two generators and a single constant power factor load. The network data and the nominal power flow solution are summarized in Table VI.

Figure 3 shows the space of active power injections at buses 2 and 3. Given that the system is lossless, the power injection at bus 1 is simply $-(P_2 + P_3)$ and consideration of another axis P_1 is unnecessary. When all the lines are in service, the power flow solution space boundary can be traced by a continuation technique [18] and is identified as Σ^0. The region enclosed by Σ^0 contains all possible power flow solutions that the present network topology (defined by line parameters) supports. The part of this region relevant to us is the quadrant having $P_2 \geq 0$ and $P_3 \leq 0$, given that
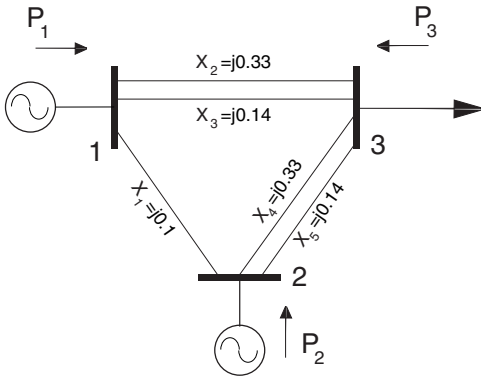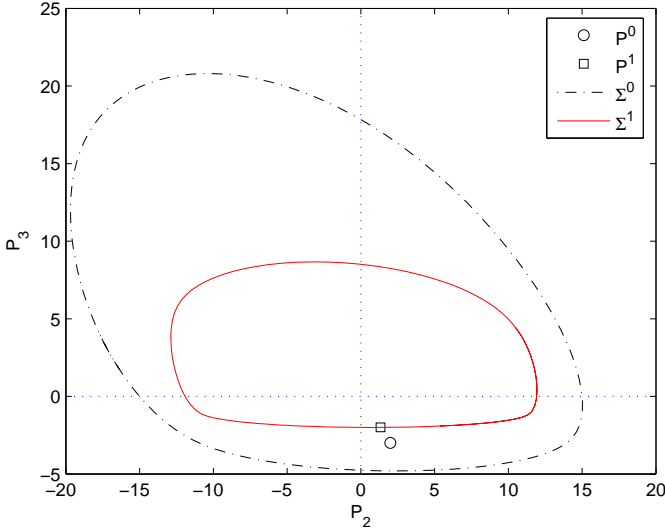
Fig. 2.   Three bus system.

Fig. 3.   Three bus system: nominal and modified power flow solution space boundary as defined by the solution in Table I.

Fig. 4.   The fourth quadrant of Figure 3.

the devices connected to buses 2 and 3 are a generator and load, respectively. Note that the nominal operating point P^0 lies within this region.

Moreover, the subset of the power flow solution space that contains solutions satisfying the voltage and angle constraints (39)–(40) defines the region of feasibility. At the nominal operating point P^0, the load bus voltage is 0.84 p.u. The lower voltage limit V_{min} is set to 0.5 p.u. in the optimization formulation (discussed later). Generator buses 1 and 2 maintain their voltages at 1 p.u. Given that there are no shunt capacitors in the network and line charging is ignored, the load bus 3 voltage would not rise above 1 p.u., effectively making the constraint $V \leq V_{max}$ unnecessary. The nominal operating point P^0 thus lies inside the region of feasibility.

Using the problem formulation (27)–(42), a few critical lines in this system are identified while ensuring that their removal will cause a failure having a severity of at least 1 p.u., or equivalently the one that will necessitate at least 1 p.u. of load shedding at bus 3. The corresponding parameter S_{min} is defined as 1. The initial guess for the solution process was obtained as described in Appendix II. The solution, summarized in Table I, identifies lines 3 and 5 as important. When
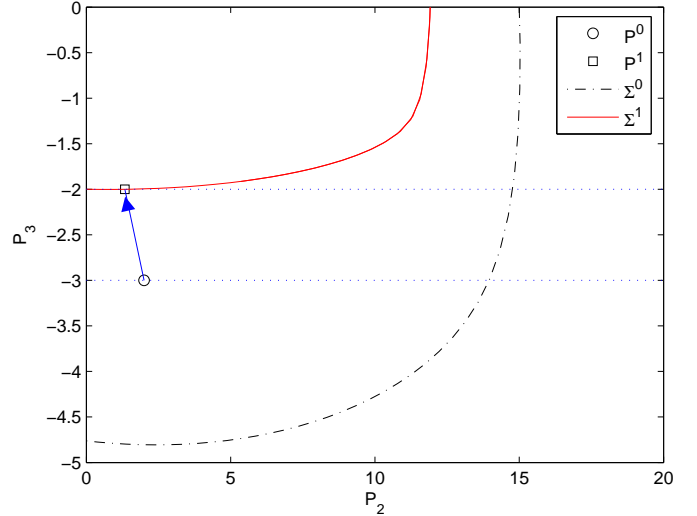
these lines are partially removed from service (as defined by their respective γ's), the load bus voltage is 0.55 p.u. and phase angles across the lines (that still remain in service) are within $\pm\pi/2$. With both voltage and angle constraints (39)–(40) inactive, the power flow Jacobian J is nontrivially singular, as discussed in Section II-B. This is shown pictorially in Figure 3. With the new network topology, the original boundary Σ^0 moves to Σ^1. Note that the original operating point P^0 lies outside this new boundary, and is now infeasible. The solution identifies point P^1 which achieves feasibility again by shedding the least possible load at bus 3. As the power flow Jacobian J is nontrivially singular, this point lies on Σ^1.

For clarity, the relevant (fourth) quadrant of Figure 3 is redrawn in Figure 4. The arrow represents the movement of the operating point from P^0 to P^1. Its projection onto the P_3 axis corresponds to the amount of load that is shed at bus 3. The optimization has obtained point P^1 lying on Σ^1 such that this projection is (locally) least possible in magnitude, while ensuring that it is at least 1 p.u. (In the present case, it is exactly 1 p.u., making the corresponding inequality constraint active.) As apparent from the figure, P^1 satisfies both these constraints. Note from Table I that due to the distributed slack bus mechanism, the generators have been redispatched in a constant proportion to their nominal values so as to accommodate the reduction of load at bus 3.

TABLE I

A THREE BUS SYSTEM SOLUTION: USING THE FORMULATION (27)–(42)

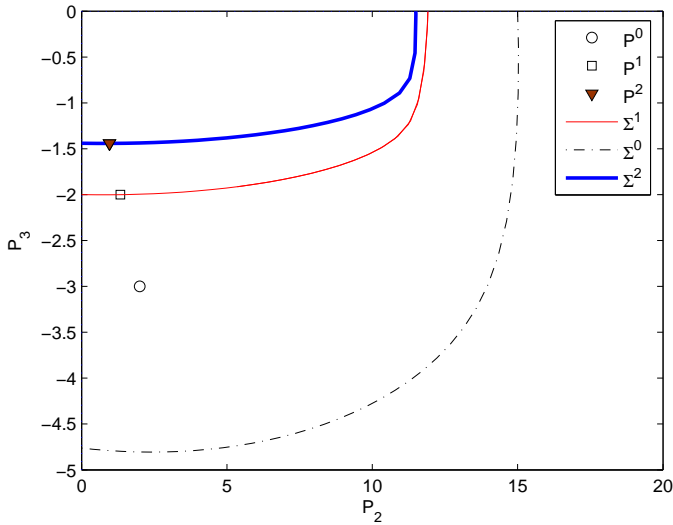| Lines identified		Load shed and generation redispatch		
Line #	γ	Bus #	P^0	P^1
3	0.67	1	1.0000	0.6667
5	1.00	2	2.0000	1.3333
		3	-3.0000	-2.0000

Fig. 5. Three bus system: nominal and modified power flow solution space boundary as defined by the solution in Table II.
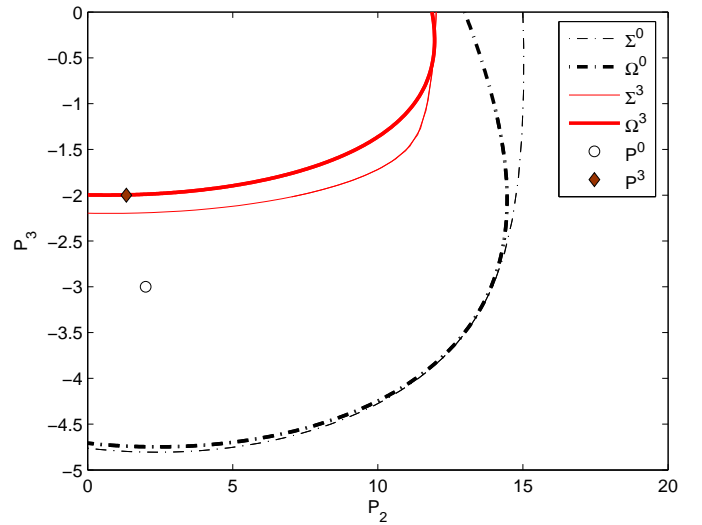

Fig. 6. Three bus system: nominal and modified power flow solution space boundary, load bus voltage constraint boundary, and optimization solution.

When the formulation (43)–(44) is used so that at most two lines are removed (i.e., with $L_{max} = 2$), lines 3 and 5 are identified again. To obtain this solution, which is summarized in Table II, the same initialization procedure as before is employed. The load bus voltage is again about 0.55 p.u. The optimization algorithm completely removes lines 3 and 5 from service in order to achieve the maximum of the objective function. This corresponds to a more severe failure (1.5582 p.u. load shed at bus 3) than the one described in Table I (1 p.u. load shed at bus 3), but it has also required (incrementally) more partial line failures.

The voltage and angle constraints are inactive for this solution too, thus making the Jacobian J nontrivially singular. It follows that the new (post load shedding) operating point P^2, as identified in Figure 5, lies on the power flow solution space boundary Σ^2 resulting from a complete removal of lines 3 and 5 from service. The operating points P^0 and P^1, and corresponding boundaries Σ^0 and Σ^1 are also shown for comparison. The power flow solution space shrinks more when both these lines are completely removed than when line 3 is only partially removed, as one would anticipate. Consequently more load is shed when a load shedding strategy moves P^0 to P^2 than to P^1. Note that the points P^0, P^1 and P^2 are collinear due to the incorporation of the distributed slack mechanism. That is, for instance, P^2 lies on Σ^2 as well as

on the line joining P^0 and the origin.

In summary, the algorithms aim to identify a few line failures (at most two) and a high blackout severity (at least 1 p.u.). A direct $N - 2$ analysis by enumeration, which is easy on this small system, can be used to validate the results obtained above. Table III enumerates the cases where any two lines are removed from service such that the power flow is infeasible. Other combinations of two simultaneous line failures do not lead to power flow infeasibility, and they are not included in the table. The least amount of load shedding required to regain feasibility is also listed in each case. Note that the removal of lines 3 and 5 achieves the highest possible severity.

When V_{min} is set to 0.7 p.u., solutions to both the optimization formulations observe a binding lower voltage constraint (39), when other parameters are set as $S_{min} = 1$ p.u. and $L_{max} = 2$. Then at the solutions, the power flow Jacobian J is *not* nontrivially singular and the new (post load shedding) operating point does not lie on the power flow solution space boundary. Instead it lies on the manifold defined by $V_3 = V_{min}$. Such solution obtained using formulation (27)–(42) is depicted graphically in Figure 6. Curve Ω^0 defines a boundary of the region where $V_3 > V_{min}$, when all lines are in service (nominal case). This region is a subset of the complete power

TABLE II

A THREE BUS SYSTEM SOLUTION: USING THE FORMULATION (43)–(44)

Lines identified		Load shed and generation redispatch		
Line #	γ	Bus #	P^0	P^1
3	1.00	1	1.0000	0.4806
5	1.00	2	2.0000	0.9612
		3	-3.0000	-1.4418

TABLE III

THE $N - 2$ ENUMERATION WITH THE THREE BUS SYSTEM

Lines removed	Severity (Load shed at bus 3)	
	p.u.	% of nominal
1, 5	0.5120	17.07%
2, 3	0.5970	19.90%
2, 5	0.6000	20.00%
3, 4	0.5970	19.90%
3, 5	1.5582	51.94%
4, 5	0.5970	19.90%

flow solution space, whose boundary is shown as Σ^0. The optimization formulation identifies lines 3 and 5, with their relaxation parameters as $\gamma_3 = 0.55$ and $\gamma_5 = 1$. With these lines (partially) removed as defined by their respective γ's, Σ^0 moves to Σ^3, and Ω^0 to Ω^3. The boundary Ω^3 encloses solutions having $V_3 > V_{min}$, at this network topology. The optimization identifies the new operating point P^3 that lies on Ω^3, thus making sure that the voltage constraint is not violated, and yet at least 1 p.u. load is shed. In the present case, exactly 1 p.u. load is shed.

We emphasize that due to the incorporation of voltage and angle constraints within our analysis, the solution feasibility boundary that we seek is not always identical with the power flow solution space boundary. It is the same as the power flow solution space boundary when load voltages and line angles are not at their limits. However, it is defined as the composite boundary of the region $V_{min} \leq V_l \leq V_{max}$ and $-\pi/2 \leq \theta_{ij} \leq +\pi/2$, when load voltage(s) V_l or line angle(s) θ_{ij} are at their limits. Mathematically, (30) defines such a feasibility boundary.

In this three bus system, no single line failure contingency results in an infeasible operation. Thus the second stage of $N - k$ enumeration study involving only lines 3 and 5 is unnecessary. Finally, it is important to note that the schematic in Figure 1 shows a space of load powers while Figures 3, 4, 5 and 6 show a complete space of all bus (nodal) powers. As there is only one load in the three bus system, the space of load powers is 1-dimensional and does not provide a significant visualization aid.

B. IEEE 30 Bus System

The IEEE 30 bus system as shown in Figure 7 is considered for the identification of lines critical for system security using the formulation discussed in Section II-D. The generators are dispatched in the original system data [27] in such a way that the system observes an active power balance within the left, right and the lower parts of the network. To emphasize some important aspects of our algorithm, the generator active power injections are modified so that there is no natural power balance in the system subsets. Table VII documents the system data that is used to obtain the results that follow.

Problem formulation (27)-(42) is used for the contingency screening. Feasible initial guesses were obtained according to the procedure described in Appendix II. The solutions were computed using the solver SNOPT [14], the AMPL modeling language [24], and the NEOS server for optimization [25], [26]. SNOPT uses a sequential quadratic programming algorithm suitable for problems with (nonlinear) objective function and is designed for both nonlinear and linear constraints with sparse derivatives. The latter is particularly attractive for the optimization problem under consideration.

An obvious (and trivial) solution to the optimization problem is the one that isolates all the generation from the loads, by removing radial lines that connect generators (and/or loads) with rest of the system. Such cases are excluded by not allowing the radial lines (in this case, lines 13, 16 and 34) to be removed from service, as our goal is to identify more subtle
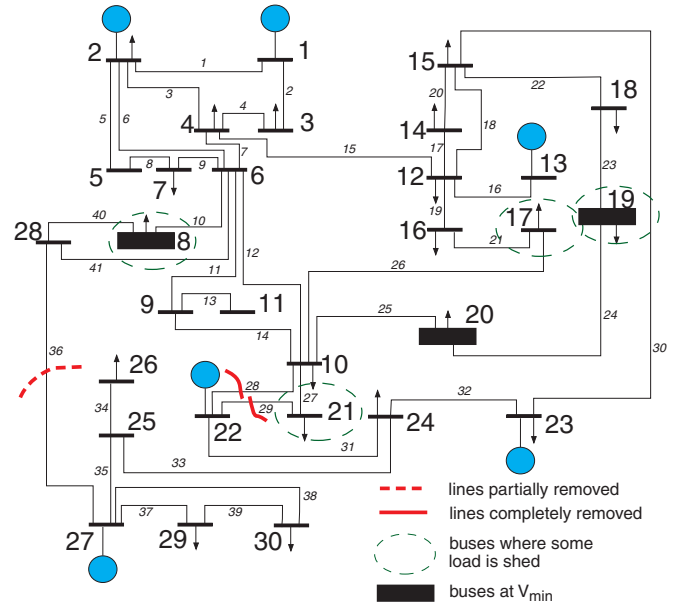

Fig. 7. Optimization solution for the IEEE 30 bus system.

solutions, that is, those not trivially revealed in the network topology.

Buses having generators attached to them are assumed to have 1.05 p.u. voltage. The base case (all lines in service and no load shedding) power flow solution results in a voltage profile such that the lowest bus voltage in the system is 0.85 p.u (at bus 8). Within the optimization framework, the limit of $V_{min} = 0.8$ p.u. is enforced on load bus voltages. This places the nominal voltage profile within the range of allowable voltage magnitudes, thus making the nominal operation feasible. Using the same argument as in Section III-A, we note that the constraint $V \leq V_{max}$ is unnecessary for this example.

Figure 7 depicts a solution based upon an initial guess provided by the initialization procedure described in Appendix II. The parameter S_{min} was set to 2 p.u. This solution identifies three transmission lines as critical ones. It also reveals that the aggregate of 2 p.u. load must be shed so as to *just* avoid a failure when these lines are removed partially from service (as defined by their respective γ's). This amounts to shedding 24.4% of the total load in the system. Table IV summarizes this solution. With lines 28 and 29 completely removed and line 36 partially removed from service, the generation rich lower region of the network is almost unable to supply loads in the other regions. This results in a sagging voltage at buses 19 and 20, and they are constrained at V_{min}. Effectively, as the solution identifies, loads at this bus and neighboring buses must be shed to maintain power flow and voltage feasibility. Recall that bus 8 had the lowest voltage at the base case power flow. It turns out that some load must be shed at this bus too, in order to avoid the overall system failure, and its voltage will sag down to V_{min} post-load shedding.

Having identified the lines whose (even partial) failure results in a severe system disturbance, one can perform the $N - k$ study by only considering those lines (where N is now

TABLE IV

THE IEEE 30 BUS SYSTEM SOLUTION

Lines identified		Load shed			Buses
Line #	γ	Bus #	p.u.	% of nominal	at V_{min}
28	1.00	8	0.3640	24.3%	8, 19, 20
29	1.00	17	0.4197	93.3%	
36	0.67	19	0.3418	72.0%	
		21	0.8750	100.0%	

TABLE V

SELECTED ENUMERATION WITH THE IEEE 30 BUS SYSTEM

Lines removed	Severity p.u.	Load shed			Buses
		Bus #	p.u.	% of nominal	at V_{min}
29	0.1136	21	0.1136	13.0%	21
28, 29	1.5239	8	0.1620	10.8%	8, 19, 20
		17	0.2524	56.1%	
		19	0.2269	47.8%	
		20	0.0076	6.9%	
		21	0.8750	100%	
29, 36	0.5138	8	0.1922	12.8%	8, 21
		21	0.3215	36.7%	
28, 29, 36	2.4700	8	0.6258	41.7%	19
		17	0.4500	100%	
		19	0.4750	100%	
		20	0.0442	40.2%	
		21	0.8750	100%	

3, rather than 41). Note that the computational burden reduces drastically, for instance, the number of combinations to analyze reduce from 820 to 3 combinations for the $N-2$ study. Table V describes the results of such an enumeration process, along with the load shedding to be performed at various buses to just avoid the otherwise impending system failure. The third column of Table V provides a load shedding strategy that will just avoid the infeasibility caused by the line removals. The net load reduction due to the load shedding is accounted for by the distributed slack mechanism. Mathematically, the process of identifying such a load shedding strategy corresponds to solving the optimization problem (9)–(13), with the constraint (13) enforced only on the lines in service.

Referring to Table V, the removal of line 29 leads to an infeasible operation as the system will not be able to hold the voltage at bus 21 at or above V_{min}[4]. About 13% of load at this bus must be shed in order to maintain feasibility. This load shedding would place the voltage at that bus at V_{min}, thus just avoiding the infeasible operation. The system operation is also infeasible when either of or both the lines 28 and 36 are removed along with line 29. For instance, when lines 28 and 29 are removed from service, a total of 1.5239 p.u. load must be shed to maintain feasibility. Voltages at buses 8, 19 and 20 would be at V_{min} when this load shedding is executed.

When all the identified lines, namely, lines 28, 29 and 36 are removed from service at a time (Table V, last row), the system gets grouped into two subsystems that are connected to each other by a single line (line 30). Recall that the group at the lower part of the network is generation rich. This results in a substantial need for load shedding in the other group (2.47 p.u., which is 30% of the total system load). Even with all the load at buses 17, 19 and 21 being shed along with partial load shedding at buses 8 and 20, the voltage at bus 19 would be as low as V_{min}.

IV. CONCLUSION

In this paper, we propose a computationally feasible approach to detect multiple contingencies resulting in a severe system failure that does not require a prohibitively expensive enumeration. This approach provides an avenue to undertake a higher order $N-k$ security analysis on a large-scale power system, in turn providing the planners and operators a deeper understanding of the system.

---

[4]A feasible operation is possible when the constraint specifying the lower limit on bus voltages is removed. Bus 21 voltage would however drop below V_{min}.

Our approach seeks to identify a few line outages such that the system will need to shed significant amount of load in order to continue a feasible operation. It is important to discuss the level of modeling detail we have used and the impact it may have on results. By incorporating a nonlinear power flow, a droop-governor-motivated distributed slack bus, and using a one-norm metric, our model is consistent with (or is more detailed than) the models used in the most closely related literature on calculating the distance to the power flow feasibility boundary. Nevertheless, it lacks a detailed representation of system dynamics and therefore our results may be optimistic if the system were to exhibit instabilities. Alternatively, neglecting fast-acting reserves and special remedial action schemes that may be in place, may make our results pessimistic. We will work in the future to add some of these features to our model. We believe the model is valuable in its present form for identifying multiple contingencies that may undergo further scrutiny, perhaps with a detailed dynamic model.

We should also comment on the practical algorithms to perform the computations outlined in this paper. While the results on our test systems reveal the effectiveness of the problem formulation, the associated nonlinear optimization problem offers many challenges for larger (continental size) problems. Due to the nonlinearity of power flow equations and other constraints, the resulting optimization problem is in general non-convex. Thus the solution obtained corresponds to a local optimum, depending upon the initial guess, the solver used and complexity of the power network under consideration. We have posed our problem in a worst-case optimization framework, but the non-convexity inherent in the model suggests that we cannot prove the result is indeed the worst case result. We would like to point out that this issue of non-convexity applies to all optimization problems that use a nonlinear model for the power grid, including traditional economic-focused optimal power flows, security margin calculations, etc., although one rarely encounters this caveat mentioned in the literature. (See

TABLE VI
THREE BUS SYSTEM DATA (NOMINAL POWER FLOW)

Bus data					Line data	
Bus #	P inject. (net), p.u.	Q inject. (net), p.u.	Ang., θ rad	Volt., V p.u.	Line #	React. X, p.u.
1	1.0000	1.7040	0.0420	1.0000	1	0.10
2	2.0000	1.7600	0.0770	1.0000	2	0.33
3	-3.0000	-2.4000	-0.1200	0.8412	3	0.14
					4	0.33
					5	0.14

[19] for a discussion of the impact of non-convexity in the context of electricity markets.)

The advantage of studying the test systems presented in this paper is that the results up to $N - 2$ can be verified by complete enumeration. The removal of lines 28 and 29 that we identify as the worst $N - 2$ case in the IEEE 30 bus example is confirmed by complete enumeration of all possible 2-line outages (excluding the ones that result in system islanding). Our approach for determining initial guesses, outlined in Appendix II, has worked well so far, but we will need to keep the issue of non-convexity in mind as we develop algorithms for large-scale systems. Special algorithms need to be developed since commercial power flows do not presently perform the calculations we have developed here. The state of the art in high performance computing provides a platform to efficiently deal with large, complex and non-convex problems. We are currently working on algorithms that can efficiently exploit such platforms.

APPENDIX I
EXAMPLE SYSTEM DATA

This appendix summarizes the data used for the three bus system and the IEEE 30 bus system, used in this paper. Tables VI and VII include the network parameters and the nominal power flow solution for these two systems respectively. Note that a few PV buses in the 30 bus system have local loads connected. Such buses are considered as PV buses with the nominal generation as the net nominal injection. In other words, they are assumed to not have any ability to perform load shedding. However a slight modification to (4)–(6) can handle the shedding of loads local to their generation.

APPENDIX II
OBTAINING FEASIBLE INITIAL GUESSES

Nonconvexity of the optimization formulation (27)–(42) demands good (feasible) initial guesses to obtain convergence. Such initial guesses can be obtained by using simplified problem formulations of the main problem. One such approach is outlined here and is used to obtain the solutions discussed in Sections III-A and III-B.

Authors discuss in [11] that the problem of contingency screening can be formulated using spectral graph partitioning approach and simplified power flow. In that formulation, all the bus voltages are assumed to be at 1 p.u., however the

nonlinearity in terms of the angles is fully considered. Solutions obtained using that approach can be processed further to provide feasible initial guesses to the optimization problem (27)–(42), as discussed below.

One can note just by inspection of the three bus system that the most severe blackout is obtained by removing lines 2, 3, 4 and 5 from the network as it will isolate the load from generation. Such a situation can be systematically identified by the graph theory based algorithm discussed in [11] for a larger system. For example, a significant blackout is obtained by removing lines 28, 29, 30 and 36 for the IEEE 30 bus system, as identified in [11]. By allowing the line parameter γ associated with only these lines to vary, the initialization process poses the problem: what is the most (locally) severe failure that can be obtained by partially removing only these lines from service? This problem can be described mathematically in an optimization framework as

$$\max_{\theta, V, z, \gamma, \mu_1, \ldots, \mu_6, \lambda} \quad e^T z, \qquad (45)$$

such that constraints (10)–(13) and (15)–(23) are satisfied along with $0 \leq \gamma \leq \gamma_{max}$ and $e^T z \geq S_{min}$. The nominal power flow solution (Table VI and Table VII) provides an initial guess for this initialization procedure. Parameter γ_{max} is set to 0.9, a value close to but less than one, and S_{min} is set to 0.5, a small positive value, to avoid graph partitioning and/or trivial solutions. (One trivial/undesired solution is $\lambda = w_0$, $\mu_1 = e$, $\mu_2, \cdots, \mu_6, z = 0$; thus making the objective function zero.) This approach has been used to obtain solutions discussed in Sections III-A and III-B.

We note that there are other ways to obtain feasible initial guesses for the optimization problem (27)–(42). One way features solving the simplified problem

$$\min_{\theta, V, z, \gamma, \mu_1, \ldots, \mu_6, \lambda} \quad \left\| e + \frac{\partial F}{\partial z}^T \lambda - \mu_1 + \mu_2 \right\|_2, \qquad (46)$$

such that constraints (10)–(13) and (16)–(23) are satisfied along with $0 \leq \gamma \leq \gamma_{max}$, $e^T \gamma \leq L_{max}$ and $e^T z \geq S_{min}$. The nominal power flow solution provides an initial guess for this initialization procedure. Random starting guesses have also produced solutions to (46).

REFERENCES

[1] "Western Electricity Coordinating Council, Operating committee handbook," III-119, Revised, 2005.

[2] "Western Electricity Coordinating Council, Operating committee handbook," III-84, Revised, 2005.

[3] F. Alvarado, I. Dobson, and Y. Hu, "Computation of closest bifurcations in power systems," *IEEE Transactions on Power Systems*, vol. 9, no. 2, pp. 918–928, May 1994.

[4] J. Arroyo and F. Galiana, "On the solution of the bilevel programming formulation of the terrorist threat problem," *IEEE Transactions on Power Systems*, vol. 20, no. 2, pp. 789–797, May 2005.

[5] C. Cañizares, "Applications of optimization to voltage collapse analysis," Panel Session: Optimization Techniques in Voltage Collapse Analysis, IEEE/PES Summer Meeting, San Diego, July 1998.

[6] ——, "Conditions for saddle-node bifurcations in AC/DC power systems," *International Journal of Electrical Power and Energy Systems*, vol. 17, no. 1, pp. 61–68, 1995.

[7] C. Cañizares, W. Rosehart, A. Berizzi, and C. Bovo, "Comparison of voltage security constrained optimal power flow techniques," in *Proceedings of the IEEE-PES Summer Meeting*, Vancouver, BC, July 2001.

[8] Q. Chen and J. McCalley, "Identifying high risk $N - k$ contingencies for online security assessment," *IEEE Transactions on Power Systems*, vol. 20, no. 2, pp. 823–834, May 2005.

[9] I. Dobson, "Observations on the geometry of saddle node bifurcation and voltage collapse in electrical power systems," *IEEE Transactions on Circuits and Systems–I: Fundamental Theory and Applications*, vol. 39, no. 3, pp. 240–243, March 1992.

[10] I. Dobson and L. Lu, "New methods for computing a closest saddle node bifurcation and worst case load power margin for voltage collapse," *IEEE Transactions on Power Systems*, vol. 8, no. 3, pp. 905–913, August 1993.

[11] V. Donde, V. López, B. C. Lesieutre, A. Pinar, C. Yang, and J. Meza, "Identification of severe multiple contingencies in electric power networks," in *Proceedings of the North American Power Symposium*, Ames, IA, October 2005.

[12] Z. Feng, V. Ajjarapu, and D. Maratukulam, "A practical minimum load shedding strategy to mitigate voltage collpase," *IEEE Transactions on Power Systems*, vol. 13, no. 4, pp. 1285–1291, November 1998.

[13] A. Flueck and J. Dondeti, "A new continuation power flow tool for investigating the nonlinear effects of transmission branch parameter variations," *IEEE Transactions on Power Systems*, vol. 15, no. 1, pp. 223–227, February 2000.

[14] P. E. Gill, W. Murray, and M. A. Saunders, "SNOPT: An SQP algorithm for large-scale constrained optimization," *SIAM J. Optim.*, vol. 12, no. 4, pp. 979–1006, 2002.

[15] S. Grijalva and P. W. Sauer, "A necessary condition for power flow Jacobian singularity based on branch complex flows," *IEEE Transactions on Circuits and Systems–I: Regular Papers*, vol. 52, no. 7, pp. 1406–1413, July 2005.

[16] ——, "Static collapse and topological cuts," in *Proceedings of the 38th Annual Hawaii International Conference on System Sciences*, Waikoloa, HI, January 2005.

[17] T. He, S. Kolluri, S. Mandal, F. Galvan, and P. Rastgoufard, *Applied Mathematics for Restructured Electric Power Systems: Optimization, Control, and Computational Intelligence*. New York: Springer, 2005, ch. Identification of Weak Locations in Bulk Transmission Systems Using Voltage Stability Margin Index.

[18] I. Hiskens and R. Davy, "Exploring the power flow solution space boundary," *IEEE Transactions on Power Systems*, vol. 16, no. 3, pp. 389–395, August 2001.

[19] B. Lesieutre and I. Hiskens, "Convexity of the set of feasible injections and revenue adequacy in FTR markets," *IEEE Transactions on Power Systems*, vol. 20, no. 4, pp. 1790–1798, November 2005.

[20] T. J. Overbye, "A power flow measure for unsolvable cases," *IEEE Transactions on Power Systems*, vol. 9, no. 3, pp. 1359–1365, August 1994.

[21] J. Salmeron, K. Wood, and R. Baldick, "Analysis of electric grid security under terrorist threat," *IEEE Transactions on Power Systems*, vol. 19, no. 2, pp. 905–912, May 2004.

[22] E. Scholtz, "Observer-based monitors and distributed wave controllers for electromechanical disturbances in power systems," Ph.D. dissertation, Massachusetts Institute of Technology, Cambridge, 2004.

[23] S. Tong and K. Miu, "A network-based distributed slack bus model for DGs in unbalanced power flow studies," *IEEE Transactions on Power Systems*, vol. 20, no. 2, pp. 835–842, May 2005.

[24] AMPL: A Modeling Language for Mathematical Programming. Information available: http://www.ampl.com/.

[25] NEOS Server for Optimization. Available: http://www-neos.mcs.anl.gov/.

[26] NEOS Guide: Optimization Software. Available: http://www-fp.mcs.anl.gov/otc/Guide/SoftwareGuide/Blurbs/sqopt_snopt.html.

[27] Power System Test Case Archive: http://www.ee.washington.edu/research/pstca/.

TABLE VII

IEEE 30 BUS SYSTEM DATA (NOMINAL POWER FLOW)

Bus data					Line data	
Bus #	P inject. (net), p.u.	Q inject. (net), p.u.	Ang., θ rad	Volt., V p.u.	Line #	React. X, p.u.
1	0.1765	0.5084	0.0387	1.0500	1	0.06
2	0.9635	2.0656	0.0390	1.0500	2	0.19
3	-0.1200	-0.0600	0.0045	0.9586	3	0.17
4	-0.3800	-0.0800	0.0017	0.9420	4	0.04
5	0.0000	0.0000	-0.0416	0.9497	5	0.20
6	0.0000	0.0000	-0.0255	0.9075	6	0.18
7	-1.1400	-0.5450	-0.0985	0.8930	7	0.04
8	-1.5000	-1.5000	-0.0842	0.8449	8	0.12
9	0.0000	0.0000	0.0345	0.9535	9	0.08
10	-0.2900	-0.1000	0.0637	0.9788	10	0.04
11	0.0000	0.0000	0.0345	0.9535	11	0.21
12	-0.5600	-0.3750	0.2047	0.9372	12	0.56
13	2.1000	1.2760	0.5080	1.0500	13	0.21
14	-0.3100	-0.0800	0.1463	0.9327	14	0.11
15	-0.4100	-0.1250	0.1721	0.9480	15	0.26
16	-0.1750	-0.0900	0.1041	0.9294	16	0.14
17	-0.4500	-0.2900	0.0474	0.9464	17	0.26
18	-0.1600	-0.0450	0.0469	0.9232	18	0.13
19	-0.4750	-0.1700	-0.0047	0.9205	19	0.20
20	-0.1100	-0.0350	0.0066	0.9326	20	0.20
21	-0.8750	-0.5600	0.1073	1.0252	21	0.19
22	1.5795	2.1958	0.1351	1.0500	22	0.22
23	1.3000	0.8515	0.3332	1.0500	23	0.13
24	-0.4350	-0.3350	0.2049	1.0080	24	0.07
25	0.0000	0.0000	0.3162	1.0110	25	0.21
26	-0.1750	-0.1150	0.2479	0.9633	26	0.08
27	2.0955	1.1650	0.4189	1.0500	27	0.07
28	0.0000	0.0000	0.0151	0.8992	28	0.15
29	-0.1200	-0.0450	0.2985	1.0050	29	0.02
30	-0.5300	-0.0950	0.2161	0.9884	30	0.20
					31	0.18
					32	0.27
					33	0.33
					34	0.38
					35	0.21
					36	0.40
					37	0.42
					38	0.60
					39	0.45
					40	0.20
					41	0.06